

Article

Identification and Expression Analysis of the FAD Gene Family in *Anoplophora glabripennis* (Coleoptera: Cerambycidae) Based on Genome-Wide Data

Xue Song ¹ , Yabei Xu ¹ , Sainan Zhang ¹, Meng Li ¹ , Yu Xing ¹, Jing Tao ^{1,*} and Fengying Han ²

¹ State Key Laboratory to Efficient Production of Forest Resources, Beijing Forestry University, Beijing 100083, China; songxue9812042021@163.com (X.S.); xuyabei0705@163.com (Y.X.); zhangsainan@bjfu.edu.cn (S.Z.); limeng_1227@bjfu.edu.cn (M.L.); xingy0714@163.com (Y.X.)

² Tongliao Forestry Pest Control Station, Inner Mongolia Autonomous Region Forestry and Grassland Bureau, Tongliao 028000, China; tlhanfengying@126.com

* Correspondence: taojing1029@hotmail.com; Tel.: +86-010-6233-6073

Abstract: Pheromones play an important role in mate choice in insects, and pheromone synthesis pathways are potential targets for the control of harmful insects, among which desaturation is of great significance in pheromone structural diversity. However, little is known about the desaturase genes regulating pheromone synthesis in Coleoptera. In this study, taking the internationally significant pest *Anoplophora glabripennis* as a research object, we identified 6 *AglaFAD* genes, all of which were mapped to the endoplasmic reticulum and shared a highly similar distribution of conserved domains. A phylogenetic analysis showed that *AglaFAD*1–2 and *AglaFAD*3–6 exerted desaturation at different positions of the acyl chain, respectively. In regard to the expression levels of these six *AglaFAD*s in both sexes, six tissues and three developmental stages were analyzed by qPCR. Combined with the chemical composition of the female pheromones that have been identified, two candidate genes, *AglaFAD*2 and *AglaFAD*5, which are specifically expressed in females, were screened, showing higher expression levels before mating and significantly decreasing after mating. It is speculated that they may be involved in the biosynthesis of contact pheromones in females. These results provide a basis for detailed functional studies of candidate genes in insect pheromone synthesis.

Keywords: *Anoplophora glabripennis*; contact pheromone; FAD gene family; genome-wide analysis; gene expression



Citation: Song, X.; Xu, Y.; Zhang, S.; Li, M.; Xing, Y.; Tao, J.; Han, F. Identification and Expression Analysis of the FAD Gene Family in *Anoplophora glabripennis* (Coleoptera: Cerambycidae) Based on Genome-Wide Data. *Forests* **2024**, *15*, 690. <https://doi.org/10.3390/f15040690>

Academic Editor: Qing-He Zhang

Received: 4 March 2024

Revised: 6 April 2024

Accepted: 9 April 2024

Published: 11 April 2024



Copyright: © 2024 by the authors. Licensee MDPI, Basel, Switzerland. This article is an open access article distributed under the terms and conditions of the Creative Commons Attribution (CC BY) license (<https://creativecommons.org/licenses/by/4.0/>).

1. Introduction

Pheromones are chemical signals that are secreted and released externally by insects for conspecific communication. Many important biological processes in insects are regulated by pheromones, such as recognition of conspecifics, courtship, and mating. Pheromones are often highly species- and sex-specific [1]. Pheromone compounds are biosynthesized in insects by a series of enzymatic reactions, including carbon chain shortening reactions, desaturation reactions, and functional group modifications [2]. Among the steps in pheromone synthesis, desaturation is of particular importance in the structural diversity of pheromones, as the wide range of substrates and stereoselectivity result in unsaturated compounds with diversities in chain length and the number, direction, and position of double bonds [3–5]. Desaturase (desat or fatty acid desaturase, FAD) introduces unsaturated double bonds at specific carbon positions in the fatty acid chain, and they are classified as $\Delta 5$, $\Delta 9$ ($C_{16} > C_{18}$), $\Delta 9$ ($C_{16} < C_{18}$), $\Delta 10$, $\Delta 11$, $\Delta 12$, $\Delta 14$, etc. based on the positions of double bonds [6].

Many studies on pheromones in Lepidoptera and Diptera have focused on the biochemical processes and genetic diversity underlying the desaturation reaction [3–5,7,8]. In *Drosophila melanogaster* (Meigen, 1830), *desat1* has $\Delta 9$ functional specificity, and *desat1*

mutations result in reduced unsaturated hydrocarbon content in the cuticles of both males and females, while males with wild-type *desat1* cannot differentiate between *desat1*-mutant males and females [9]. Furthermore, *desatF* plays a key role in the synthesis of dienophiles in *D. melanogaster* and is only expressed in females. RNA interference targeting *desatF* leads to a decrease in female epidermal diolefins and an increase in mono-olefins, as well as an increase in mating duration and a decrease in the number of courtship and mating attempts by males [10,11]. *Ctenopseustis obliquana* (Walker, 1863) utilizes $\Delta 5$ dehydrogenase, encoded by *desat7*, to catalyze the formation of Z5–14:OAc from 14:Acid [12]. *Trichoplusia ni* (Hübner, 1802) uses $\Delta 11$ dehydrogenase to produce Z11–16:OAc and Z11–18:OAc, while *Helicoverpa zea* (Boddie, 1850) catalyzes the synthesis of Z9–16:OAc and Z9–18:OAc using $\Delta 9$ dehydrogenase [13]. These studies indicate that FAD affects the structure, content, and sex-biased expression of insect pheromones, thereby affecting courtship and mating behavior.

Anoplophora glabripennis (Motschulsky, 1853) originated in China and the Korean Peninsula and was introduced to the United States and Canada in the 1990s, followed by France, Britain, and other European countries [14–18]. In China, it is widespread, ranging from 100° to 127° E longitude, 21° to 43° N latitude in the eastern area of the distribution, with a recent trend toward expansion to high-altitude, high-latitude areas in Xinjiang, Tibet, Heilongjiang, and other places becoming apparent [19,20]. *A. glabripennis* mainly harms willow, poplar, mulberry, elm, and other forest trees. Its larvae feed on the xylem of the main trunk of the host plant, forming permanent cavities and defects in the tree and seriously affecting tree growth and survival, causing significant losses to forestry production [17,21–23].

Owing to the harmful effects of *A. glabripennis*, its large host range, and its activity during the adult stage making control difficult, the use of pheromones to detect and control adults has become a fast and environmentally friendly means of prevention and control. Therefore, the identification of chemical substances that affect mating behavior is a major area of research [24,25]. Ginzel and Hanks [26] pointed out that Cerambycidae completes its mating and reproduction behaviors in a three-step approach. First, both sexes are attracted to the volatile substances of the host plant and localize near the host location. Then, host volatiles and male aggregation pheromones work together to attract both sexes. Lastly, both sexes come into physical contact, and the males are stimulated to mate by the female contact pheromones. However, in 2012, Wickham et al. [27] suggested that long-range pheromones released by females likely play a role, reporting the following “four-step approach” to mating and reproduction: (1) unmated females are attracted by the host plant, (2) long-range pheromones released by females and host volatiles work together to attract males, (3) both sexes are attracted to male aggregation pheromones, and (4) female contact pheromones attract males, resulting in mating. These previous studies indicate that the contact pheromone of female Cerambycidae is likely the decisive substance for the completion of mating behavior. Li et al. [28] detected a contact pheromone in the wing base of female *A. glabripennis* and proved that male adults seek mates with the help of contact pheromones produced by females through field experiments. Using GC-MS, Zhang et al. [29] found that the contact pheromone components released by *A. glabripennis* females are a series of long-chain hydrocarbons (specifically (Z)-9-tricosene, (Z)-9-pentacosene, (Z)-7-pentacosene, (Z)-9-heptacosene, and (Z)-7-heptacosene (at a ratio of 1:2:2:8:1)) and elicit courtship and mating behaviors in males. Among these, Z9-tricosene is also a sex pheromone component in *Musca domestica* (Linnaeus, 1758), showing a similar synthetic pathway to that in lepidopteran insects; in particular, the double bond is introduced into the stearic acid 9 position in the presence of $\Delta 9$ -DES, followed by carbon chain extension and decarboxylation reactions [30,31]. In *Spodoptera litura* (Fabricius, 1775), interference with the *Des5* gene can effectively reduce the production of female sex pheromones [32]. Since the five main components of the female contact pheromone of *A. glabripennis* are all monounsaturated olefins, we hypothesized that FAD, which is involved in pheromone synthesis in vivo, has female-biased expression, displaying an elevated expression at sexual maturity.

Using molecular biology methods, we analyzed the spatial and temporal expression patterns of *FAD* genes in *A. glabripennis* to better understand the functions of genes that are highly expressed in females and to find the key genes affecting contact pheromone synthesis. Six *FAD* genes were screened and identified in *A. glabripennis*, and their gene structure, basic physical and chemical properties, and phylogeny were analyzed. Furthermore, the expression profiles of *AglaFADs* in different sexes, tissues, and developmental stages were analyzed by qPCR. The results of this study reveal the molecular features and expression characteristics of the *AglaFAD* gene family, suggesting that the *AglaFADs* play a key role in contact pheromone synthesis and provide a basis for subsequent in-depth functional assays, as well as for the synthesis of novel inhibitors or pheromones for the effective control of *A. glabripennis*.

2. Materials and Methods

2.1. Identification and Analysis of the *AglaFAD* Gene Family

2.1.1. Identification of *FAD* Genes in the *A. glabripennis* Genome

The genome sequence data for *A. glabripennis* were obtained from the NCBI database (<https://www.ncbi.nlm.nih.gov/>, accessed on 3 April 2023). Using published *FAD* protein sequences for *M. domestica* and *D. melanogaster* as templates, a BlastP search was performed against the genome of *A. glabripennis* to collect all sequences with an E-value below 1×10^{-5} . Subsequently, the Hidden Markov Model (HMM) profile for a FA_desaturase conserved domain (PF00487) was downloaded from the Pfam database (<http://pfam-legacy.xfam.org/>, accessed on 8 April 2023) and used to search against the protein sequence data for *A. glabripennis* using HMMER 3.0 (The Eddy Laboratory, Cambridge, MA, USA) to acquire putative *A. glabripennis* *FAD* genes with an E-value below 0.05. The putative *A. glabripennis* *FAD* genes acquired from both the BlastP search and HMMER 3.0 search were combined, and the redundant sequences were removed. The NCBI Conserved Structural Domain Database (<https://www.ncbi.nlm.nih.gov/Structure/cdd/wrpsb.cgi>, accessed on 10 April 2023) was used to confirm the presence of a conserved structural domain in all putative *A. glabripennis* *FAD* proteins.

2.1.2. Sequence Alignment and Phylogenetic Analysis

The number of amino acids (AA), isoelectric points (pI), molecular weights (MWs), instability index (II), and grand average of hydropathicity (GRAVY) of all *AglaFAD* proteins were calculated in the ExPasy website (<https://web.expasy.org/protparam/>, accessed on 15 April 2023). Transmembrane regions were predicted using TMHMM2.0 (<https://services.healthtech.dtu.dk/service.php?TMHMM-2.0>, accessed on 15 April 2023). Subcellular localization was predicted using WoLF PSORT (<https://wolfsort.hgc.jp/>, accessed on 17 April 2023).

The amino acid sequences of *FADs* listed in Table 1 were derived from the NCBI database (<https://www.ncbi.nlm.nih.gov/>, accessed on 15 April 2023), and *FAD* information for most species was referenced from previous studies [33], with all sequences being aligned using Clustal W1.81 (Conway Institute UCD Dublin, Dublin, Ireland). A phylogenetic tree was constructed using the neighbor-joining method with 1000 bootstrap replicates. The phylogenetic tree was visualized using EvolView (<https://www.evolgenius.info/evolview/>, accessed on 18 April 2023). *AglaFAD* sequences were visualized using ESPript 3.0 (<https://esprict.ibcp.fr/ESPript/ESPript/>, accessed on 18 April 2023).

Table 1. Overview of FADs included in phylogenetic analysis.

Species	FAD Name	Protein Accession
<i>Ostrinia nubilalis</i>	OnubZ/E14	AAL35330
<i>Ostrinia scapulalis</i>	OscFAD14	BAE97679
<i>Choristoneura parallela</i>	CparZ9	AAQ12887
<i>Lampronia capitella</i>	LcapZ9	ABX71627
<i>Helicoverpa assulta</i>	HassGATD	AAM28480
<i>Lampronia capitella</i>	LcapNF	ABX71629
<i>Helicoverpa assulta</i>	HassZ9	AAM28481
<i>Ascotis selenaria cretacea</i>	Asel	BAF97042
<i>Planotortrix octo</i>	PoctZ9	AAF73073
<i>Argyrotaenia velutinana</i>	AvelZ9	AAF44709
<i>Choristoneura rosaceana</i>	CrosZ9	AAN39697
<i>Ostrinia nubilalis</i>	OnubZ9	AAF44710
<i>Dendrolimus punctatus</i>	DpunZ/E9	ABX71810
<i>Bombyx mori</i>	Bmor	NP_001036971
<i>Helicoverpa zea</i>	HzeaZ11	AAF81787
<i>Trichoplusia ni</i>	TniZ9	AAB92583
<i>Spodoptera littoralis</i>	SlitZ9-2	AAQ74257
<i>Helicoverpa assulta</i>	HassZ9-2	AAM28484
<i>Dendrolimus punctatus</i>	Dpun	ABX71813
<i>Ostrinia furnacalis</i>	OfurZ9	AAL27034
<i>Bombyx mori</i>	Bmor-2	NP_001037018
<i>Argyrotaenia velutinana</i>	AvelZ/E11	AAL16642
<i>Dendrolimus punctatus</i>	DpunZ/E11	ABX71809
<i>Mamestra brassicae</i>	MbraZ11	ABX90049
<i>Thaumetopoea pityocampa</i>	TpitZ11-13	ABO43722
<i>Ostrinia furnacalis</i>	OfurZ/E11	AAL32060
<i>Ostrinia nubilalis</i>	OnubZ/E11	AAL35331
<i>Choristoneura rosaceana</i>	CrosNF	AAN39698
<i>Bombyx mori</i>	Bmor-3	NP_001036914
<i>Choristoneura parallela</i>	CparNF	AAN39693
<i>Choristoneura rosaceana</i>	CrosZ/E11	AAN41250
<i>Helicoverpa zea</i>	HzeaZ9	AAF81788
<i>Bombyx mori</i>	Bmor-4	NP_001040141
<i>Ostrinia brumata</i>	Obru-TerDesat	AEH95845
<i>Planotortrix octo</i>	PoctZ10	AAG54077
<i>Antheraea pernyi</i>	AperZ11	ADO85596
<i>Drosophila melanogaster</i>	Dmel1	AAB17283
<i>Drosophila melanogaster</i>	Dmel2	CAB52474
<i>Dendroctonus ponderosae</i>	Dpon1	XP019762450
<i>Dendroctonus ponderosae</i>	Dpon2	XP019762452
<i>Dendroctonus ponderosae</i>	Dpon3	XP019762451
<i>Dendroctonus ponderosae</i>	Dpon4	XP019755346
<i>Anoplophora glabripennis</i>	AglaFAD1	XP_018565922.1
<i>Anoplophora glabripennis</i>	AglaFAD2	XP_018576960.1
<i>Anoplophora glabripennis</i>	AglaFAD3	XP_023313032.1
<i>Anoplophora glabripennis</i>	AglaFAD4	XP_018579075.1
<i>Anoplophora glabripennis</i>	AglaFAD5	XP_018579055.1
<i>Anoplophora glabripennis</i>	AglaFAD6	XP_023310323.1

2.1.3. Structural Characterization of *AglaFADs*

The structure information of 6 *AglaFAD* genes was acquired from the gff file of the *A. glabripennis* genome and the exon–intron structure of *AglaFADs* was visualized using TBtools. The conserved motifs of *AglaFAD* protein sequences were analyzed using MEME (<https://meme-suite.org/meme/tools/meme>, accessed on 18 April 2023), with the maximum motif search value set to 10.

2.1.4. Chromosomal Locations of *AglaFADs*

Locus information was organized and *AglaFAD* genes were mapped on chromosomes using TBtools-II (C.C., Guangzhou, China).

2.2. Tissue Expression of *AglaFADs*

2.2.1. Insect Collection and Processing

In June 2023, the larvae and pupae of *A. glabripennis* were collected from a willow forest next to the Longwangtan Reservoir in Jiayuguan City, Gansu Province (39°47' N, 98°17' E), and brought to the laboratory in Beijing, where they were reared in a rearing box with fresh willow twig segments. The twig segments were replaced every 2–3 days. Water-soaked cotton wool was placed in the rearing box to provide moisture. The temperature was controlled at 25 ± 1 °C. Three pairs of male and female insects were selected at primary eclosion, sexual maturity (feeding 12–14 days after feathering), and after mating, while different tissues (head, antennae, thorax, wing, leg, and gonad) were cut out and stored in a refrigerator at −80 °C until RNA extraction.

2.2.2. RNA Extraction and qPCR Analysis of *AglaFADs*

Total RNA extraction was performed according to the instructions provided with the EASYspin Plus Tissue/Cell RNA Rapid Extraction Kit RN28 (Aidlab Biotechnologies Co., Ltd., Beijing, China). The concentration and quality of RNA were verified using the UV spectrophotometer NanoDrop 8000 (Thermo, Waltham, MA, USA) and 1.2% agarose gel electrophoresis. Reverse transcription was performed using the PrimeScript RT Reagent Kit with a gDNA Eraser (No. RR047A; TaKaRa, Dalian, China), and first-strand cDNA was synthesized with 1 µg of total RNA. Specific primers for qPCR were designed within the CDS of each gene using Primer3Plus (<https://www.primer3plus.com/>, accessed on 2 September 2023), and the primer sequences for six *AglaFADs* and one β -Actin are shown in Table 2. Quantitative real-time PCR (qRT-PCR) was performed on the CFX96TM Real-time system (Bio-Rad, Hercules, CA, USA) and SYBR Premix Ex Taq (No. RR820A; TaKaRa). The reaction mixture was as follows: SYBR Premix Ex Taq 6.25 µL, cDNA template 1 µL, primers 0.5 µL, and 4.25 µL ddH₂O to supply the volume to 12.5 µL. The amplification program was set as follows: Pre-denaturation at 95 °C for 30 s, then 40 cycles, including 95 °C for 5 s, 60 °C for 30 s, 95 °C for 10 s, while the melting procedure was the default of the instrument. β -Actin was the internal reference gene. All treatments involved 3 biological replicates per sample and 3 technique replicates, and relative expression levels were analyzed using the $2^{-\Delta\Delta CT}$ method.

Table 2. qPCR primers for the *AglaFAD* gene family.

Gene Name	Forward Primer	Reverse Primer
<i>AglaFAD1</i>	5'-TTCGTGCCGAGGATACGATG-3'	5'-AAGCCCTATGTGACCACAGC-3'
<i>AglaFAD2</i>	5'-TCACACCGCTACGATGCTT-3'	5'-ATGTTGCCTGTGATCTCGCA-3'
<i>AglaFAD3</i>	5'-CTCTGGTCTCATCGTGCTT-3'	5'-TTCGCTGAATTTATGGTGG-3'
<i>AglaFAD4</i>	5'-TGGTGGATTGGGTGTCACTG-3'	5'-GAATCCGCGTTTGGCATTGT-3'
<i>AglaFAD5</i>	5'-AGAGGTGGTTGCAAAAGCCA-3'	5'-TGCCTTGTAGGAACGATGGG-3'
<i>AglaFAD6</i>	5'-TGCTTTAAATGCCACATGGTTAGT-3'	5'-TGCAGCAGAGAAGTTTACTG-3'
β -Actin	5'-ACATCAAGGAGAACTCTGCTACG-3'	5'-CTTCATGATGGAGTTGTAGGTGGT-3'

2.2.3. Statistical Analysis

In this study, the expression levels of 6 *AglaFADs* in 6 tissues of males and females were investigated, and the changes in their expression levels in the 3 developmental stages of females were further explored. Statistical analyses were performed by one-way analysis of variance (ANOVA) and least-significant difference (LSD) tests using SPSS 27.0 (IBM Corp., Armonk, NY, USA). Additionally, $p < 0.05$ indicated a statistically significant difference. Gene expression levels in female legs were used as controls. Quantitative data are expressed

as means \pm standard error of mean (SEM). The results were visualized with GraphPad Prism 9.5.0 (GraphPad Software Inc., San Diego, CA, USA).

3. Results

3.1. Genome-Wide Identification of *AglaFADs*

Six *AglaFAD* genes were identified based on *A. glabripennis* protein sequence data found through BlastP and HMM searches. They encoded the proteins of 279–378 amino acids with predicted molecular weights of 32,373.85–43,133.42 Da. Four proteins had isoelectric points (pI) greater than seven and were basic; two proteins had isoelectric points (pI) less than seven and were acidic. Two proteins had instability coefficients (II) higher than 40 and were unstable. Four proteins with instability coefficients (II) lower than 40 were stable. The total average hydrophilicity (GRAVY) of all proteins was less than 0, indicating that they were hydrophilic (Table 3).

Table 3. Physicochemical properties of the *AglaFAD* gene family.

<i>AglaFAD</i> Member	Protein ID	AA	MW (Da)	pI	II	Transmembrane Domain	Subcellular Localization	GRAVY
<i>AglaFAD1</i>	XP_018565922.1	374	43,133.42	6.76	39.26	5	Endoplasmic reticulum.	−0.192
<i>AglaFAD2</i>	XP_018576960.1	378	43,106.85	8.66	32.29	5	Endoplasmic reticulum.	−0.032
<i>AglaFAD3</i>	XP_023313032.1	349	40,383.17	6.40	30.63	4	Endoplasmic reticulum.	−0.131
<i>AglaFAD4</i>	XP_018579075.1	349	40,339.53	8.23	40.83	4	Endoplasmic reticulum.	−0.113
<i>AglaFAD5</i>	XP_018579055.1	349	40,323.44	8.19	42.89	4	Endoplasmic reticulum.	−0.134
<i>AglaFAD6</i>	XP_023310323.1	279	32,373.85	7.01	36.06	2	Endoplasmic reticulum.	−0.190

3.2. Phylogenetic Analysis and Multiple Sequence Alignment of *AglaFADs*

To infer the evolutionary relationship among *AglaFADs* and other species, phylogenetic analyses were conducted based on the six *AglaFADs* and *FADs* of other Lepidoptera, Hymenoptera, and Coleoptera insects listed in Table 1. As shown in Figure 1 (sequences listed in Supplementary Materials), the phylogenetic tree consisted of 48 amino acid sequences from 22 species, which were divided into five groups ($\Delta 14$, $\Delta 11$, $\Delta 9$ (C16 > C18), $\Delta 9$ (C16 < C18), $\Delta 9$ (C16–C26)), among which, $\Delta 11$ and $\Delta 9$ (C16 > C18) had a large number of amino acid sequences, 15 and 12, respectively. We also found that the *AglaFADs* were always present on the branch where the *FADs* of *Dendroctonus ponderosae* (Hopkins, 1902) were, indicating that the *FADs* of *A. glabripennis* were more closely related to the *FADs* extracted from *D. ponderosae*. The sequence lengths of *AglaFADs* and *Dpons* in $\Delta 14$ were basically greater than 370 bp, and most of the *AglaFADs* and *Dpons* in $\Delta 9$ (C16–C26) were less than 370 bp. All *AglaFADs* had three conserved histidine-rich structural regions (His I, His II, and His III), which are conserved structural regions unique to the First Desaturase subfamily and function in importing the first pair of double bonds into the saturated acyl chain (Figure 2).

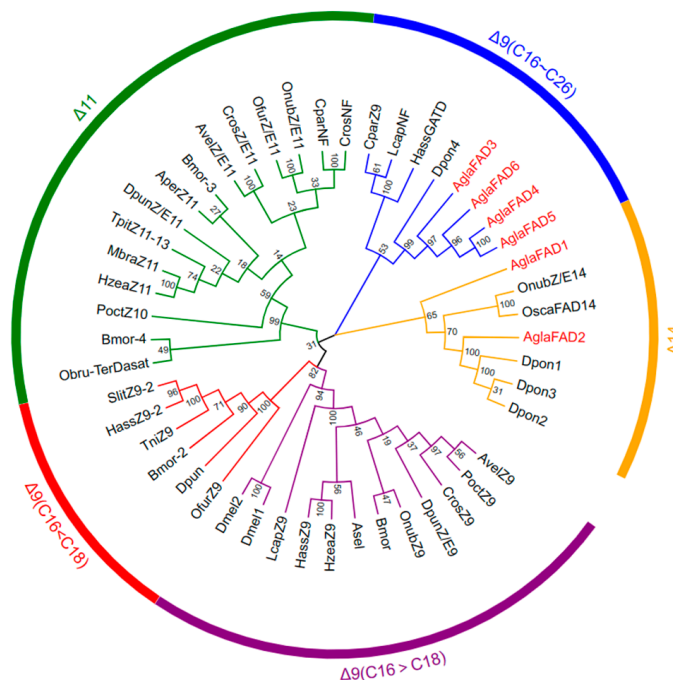


Figure 1. Phylogenetic tree of FAD proteins from different species. Different colors indicate different FAD branches: $\Delta 14$ (orange), $\Delta 11$ (green), $\Delta 9$ (C16 > C18) (purple), $\Delta 9$ (C16 < C18) (red), $\Delta 9$ (C16–C26) (blue), and the FADs of *A. glabripennis* are highlighted in red (node support based on 1000 bootstrap replications is shown).

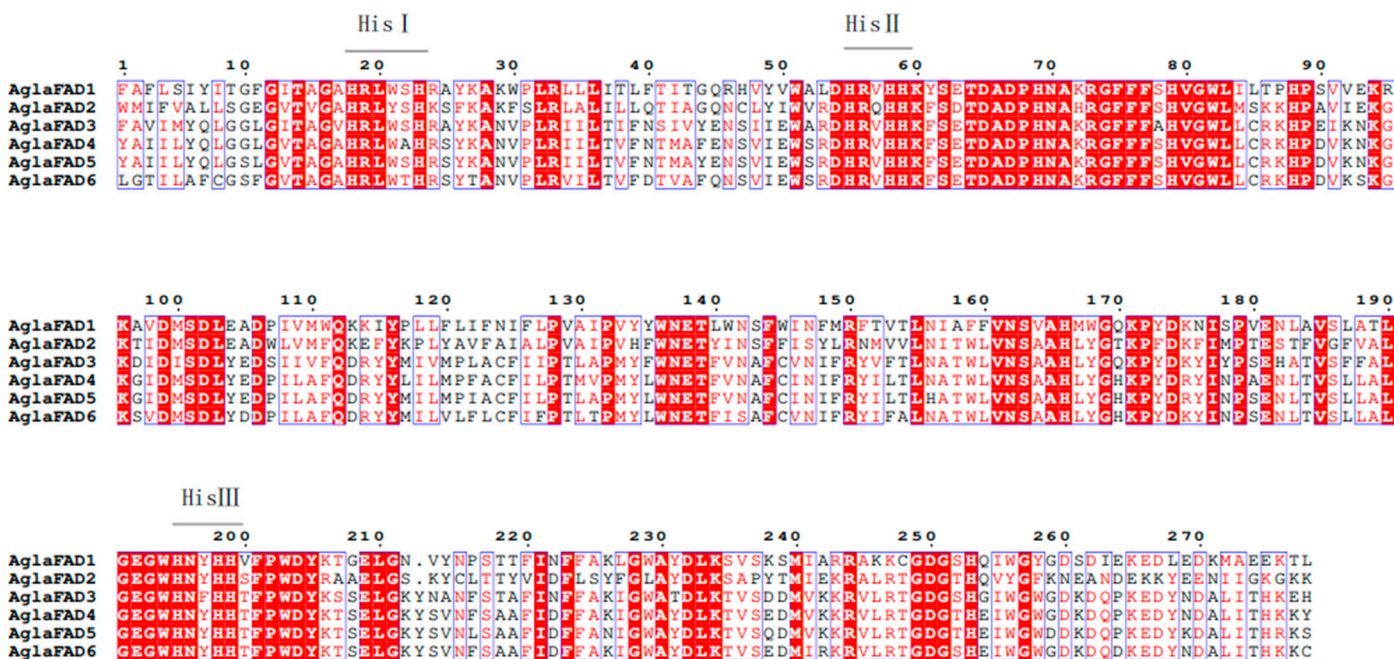


Figure 2. Multiple sequence alignment of AglaFADs. The gray lines above the sequence represent HisI, HisII, and HisIII, which are conserved histidine-rich structural regions.

3.3. Structural Analysis of AglaFADs

Based on the phylogenetic analysis, the exon–intron structures and conserved motifs of *AglaFADs* were further analyzed. As shown in Figure 3, all *AglaFADs* contained four–five introns, except *AglaFAD6*, which had two introns, indicating that the gene structure was relatively conserved. Ten conserved motifs of *AglaFADs* were identified using the MEME

online tool. AglaFAD1–6 had six same conserved motifs and minor differences in the composition of other motifs. Moreover, the three conserved histidine-rich structural regions of all members were located in motif5, motif1, and motif2 (Figure 4), and the histidine domains of FADs can bind to Fe ions to form the catalytic center of FADs, which is the structural basis for the biological functions of FADs [34,35]. Using the NCBI conserved domain database, all six AglaFADs were searched for the Δ9-fatty acid desaturase analog structural domain (Delta9-FADs-like) (Figure 5).

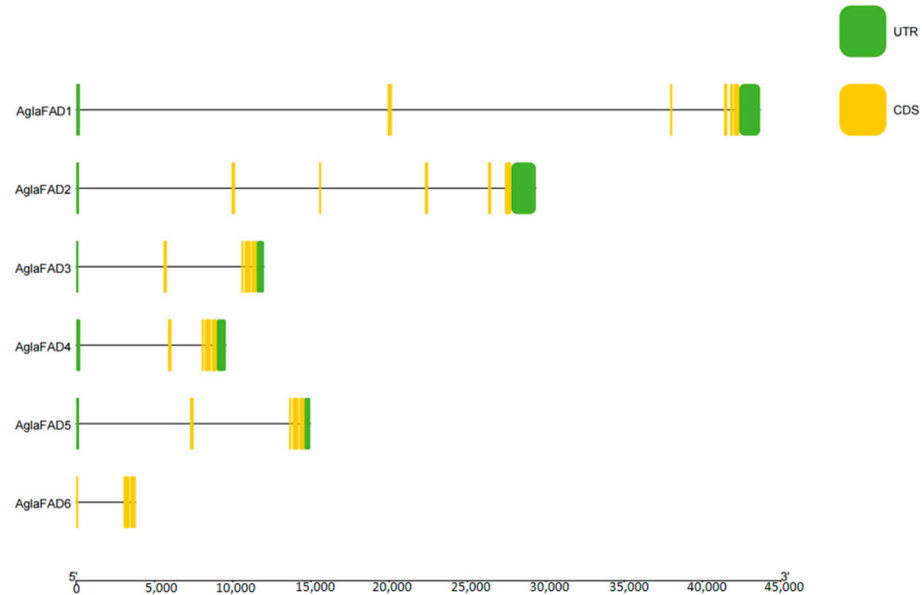


Figure 3. Exon–intron structures of *AglaFADs*. Green boxes, black lines, and yellow boxes represent untranslated regions, intron, and CDS, respectively.

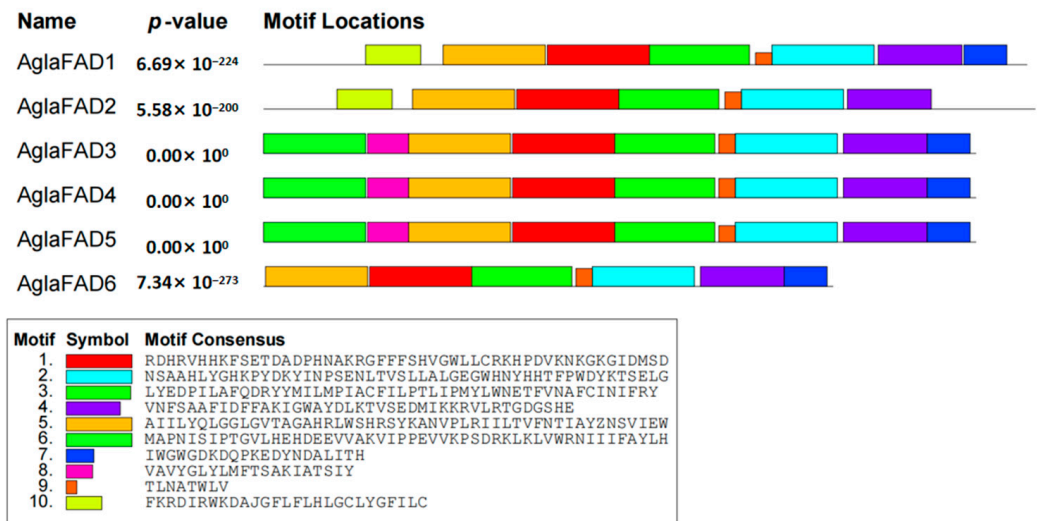


Figure 4. Analysis of the conserved motifs of *AglaFADs*. Boxes with different colors represent different motifs. The number in the box represents the motif number and provides a detailed description of the motif.

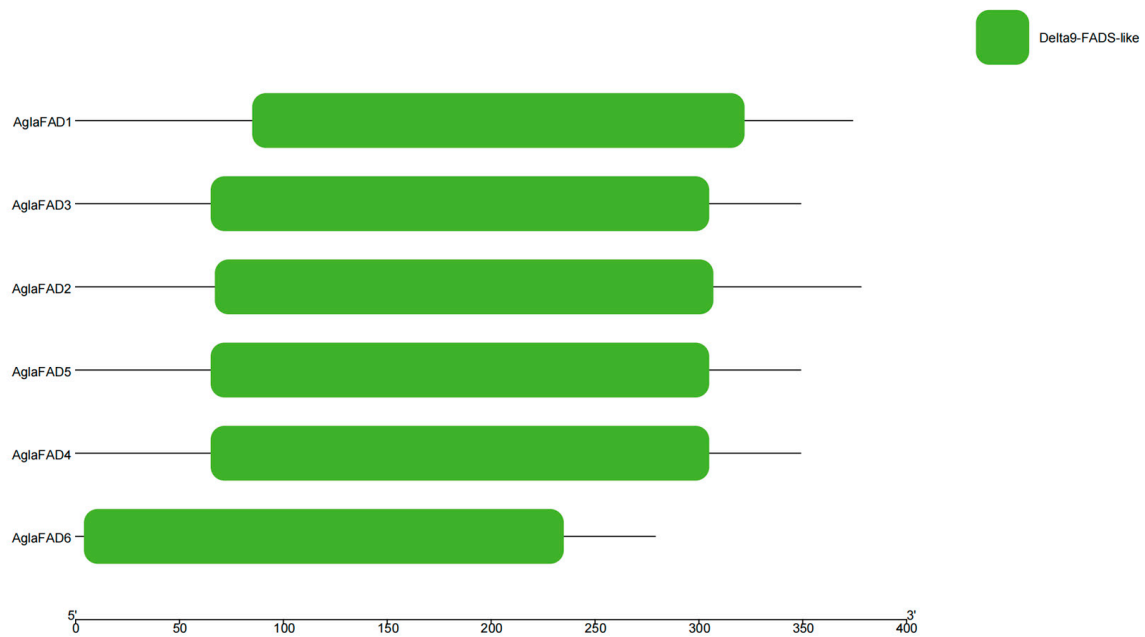


Figure 5. Conserved structural domain in the AglaFAD gene family. The green color represents the Δ^9 -fatty acid desaturase analog structural domain (Delta9-FADS-like).

3.4. Analysis of Chromosomal Locations of AglaFADs

With respect to chromosomal localization (Figure 6), *AglaFAD4*, *5*, and *6* were located in clusters on the same chromosome, while *AglaFAD1*, *2*, and *3* were located on three different chromosomes.

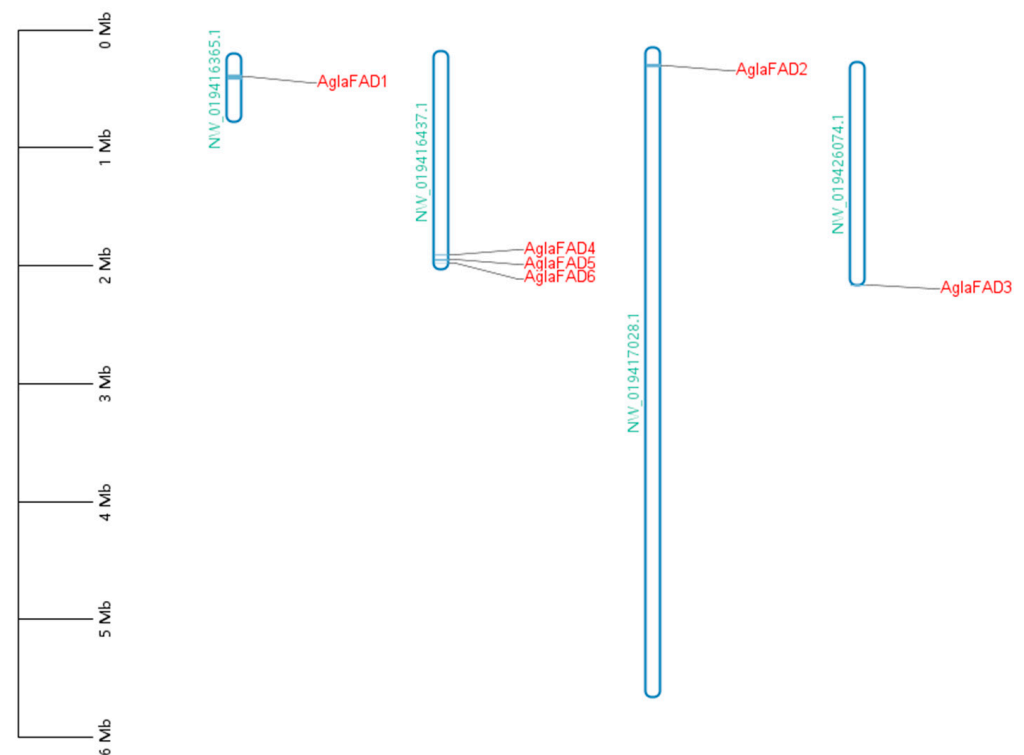


Figure 6. Chromosome mapping of FAD family members in *A. glabripennis*. Gray lines, positions of each member of the FAD gene family on the chromosome. The green font on the left of the chromosome is the chromosome name. The vertical scale indicates the chromosome size.

3.5. Expression Analysis of *AglaFADs*

3.5.1. Expression of *AglaFADs* in Males and Females at Sexual Maturity

RT-qPCR was employed to analyze the expression patterns of *AglaFADs* in six tissues (head, antennae, thorax, wing, leg, and gonad) in both sexes at sexual maturity (Figure 7). *AglaFAD2* and *AglaFAD5* showed female-biased expression, and *AglaFAD3* showed male-biased expression, suggesting that *AglaFAD3* might be involved in the synthesis of a male-specific metabolite or gonadal development. The other three *AglaFAD* genes showed no obvious sex-biased expression. *AglaFAD1* displayed few differences in expression among the same tissues in males and females, and *AglaFAD4* and *AglaFAD6* showed higher expression levels in the head, wing, and gonads than in other tissues in both sexes. These genes might act as housekeeping genes to regulate basic metabolic homeostasis. Both *AglaFAD2* and *AglaFAD5* were highly expressed in the wings and gonads of females, with high expression levels of *AglaFAD2* in the antennae and *AglaFAD5* in the head, suggesting that they might be key genes in contact pheromone biosynthesis.

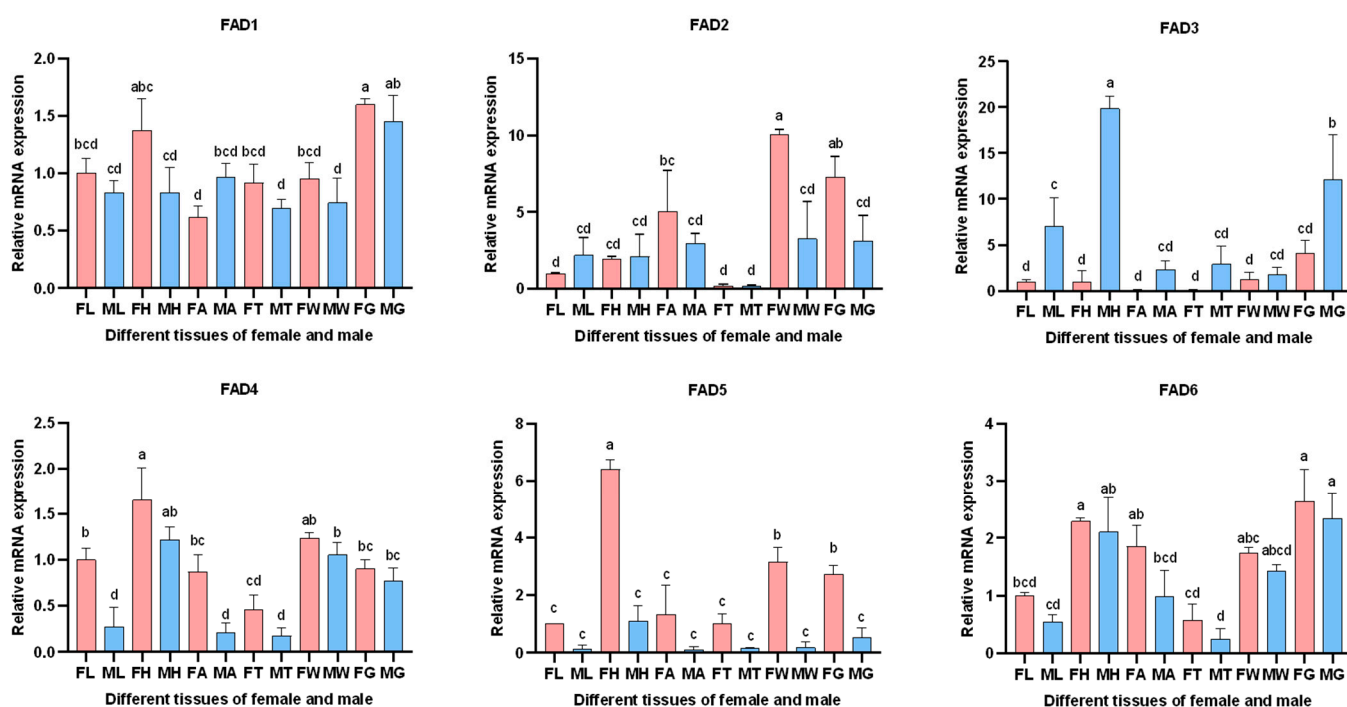


Figure 7. Expression profiles of *AglaFAD* genes in different tissues. Note: FL, female leg; ML, male leg; FH, female head; MH, male head; FA, female antennae; MA, male antennae; FT, female thorax; MT, male thorax; FW, female wing; MW, male wing; FG, female gonad; MG, male gonad. Gene expression of FAD-FL was used as control, and relative expression levels are expressed as means \pm standard error of mean (SEM). Letters above the error bar indicate significant differences between 12 tissues ($p < 0.05$, LSD).

3.5.2. Expression of *AglaFADs* at Different Developmental Stages in the Wings and Gonads of Females

RT-qPCR was used to detect the expression of *AglaFADs* in the wings of females during three developmental periods (primary eclosion, sexual maturity, and after mating) (Figure 8). The expression levels of *AglaFAD2* and *AglaFAD5* in the wings of females tended to increase and then decrease, rising to the highest level during sexual maturity and then decreasing significantly after mating. This trend may be related to differences in the demand for contact pheromones by females at different periods. The expression levels of *AglaFAD3* did not differ significantly among periods. *AglaFAD1*, *AglaFAD4* and *AglaFAD6* expression levels were relatively low and increased progressively with age prior to sexual

maturity; after mating, the relative expressions of *AglaFAD1* and *AglaFAD6* decreased slightly, while the expression of *AglaFAD4* increased significantly.

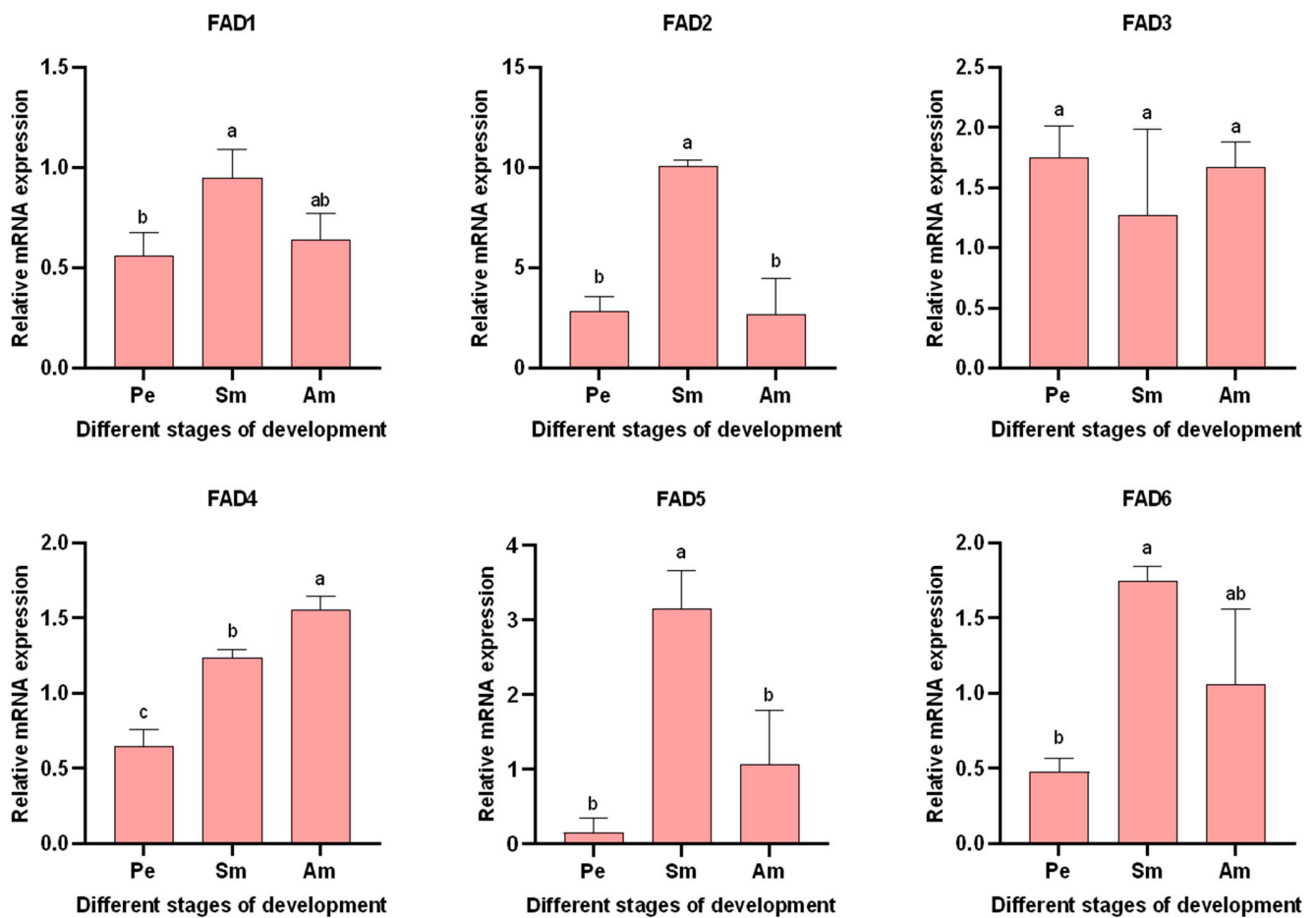


Figure 8. Expression profiles of *AglaFAD* genes in different stages of development. Note: Pe, primary eclosion; Sm, sexual maturity; Am, after mating. Letters above the error bars indicate significant differences between 3 stages ($p < 0.05$, LSD).

RT-qPCR was used to detect the expression of *AglaFADs* in the gonads of females among the three developmental periods (Figure 9). The trends in the relative expression of *AglaFAD5* in the gonads of females was similar to that in the wings, characterized by an initial increase, followed by a decrease during development. *AglaFAD2* was relatively highly expressed during primary eclosion, indicating that it is possible that *AglaFAD2* is involved in early gonadal development. *AglaFAD1*, 3, and 6 showed no significant differences in expression among stages. *AglaFAD4* increased significantly, with relatively low expression in the early stages of development and stable levels after sexual maturity.

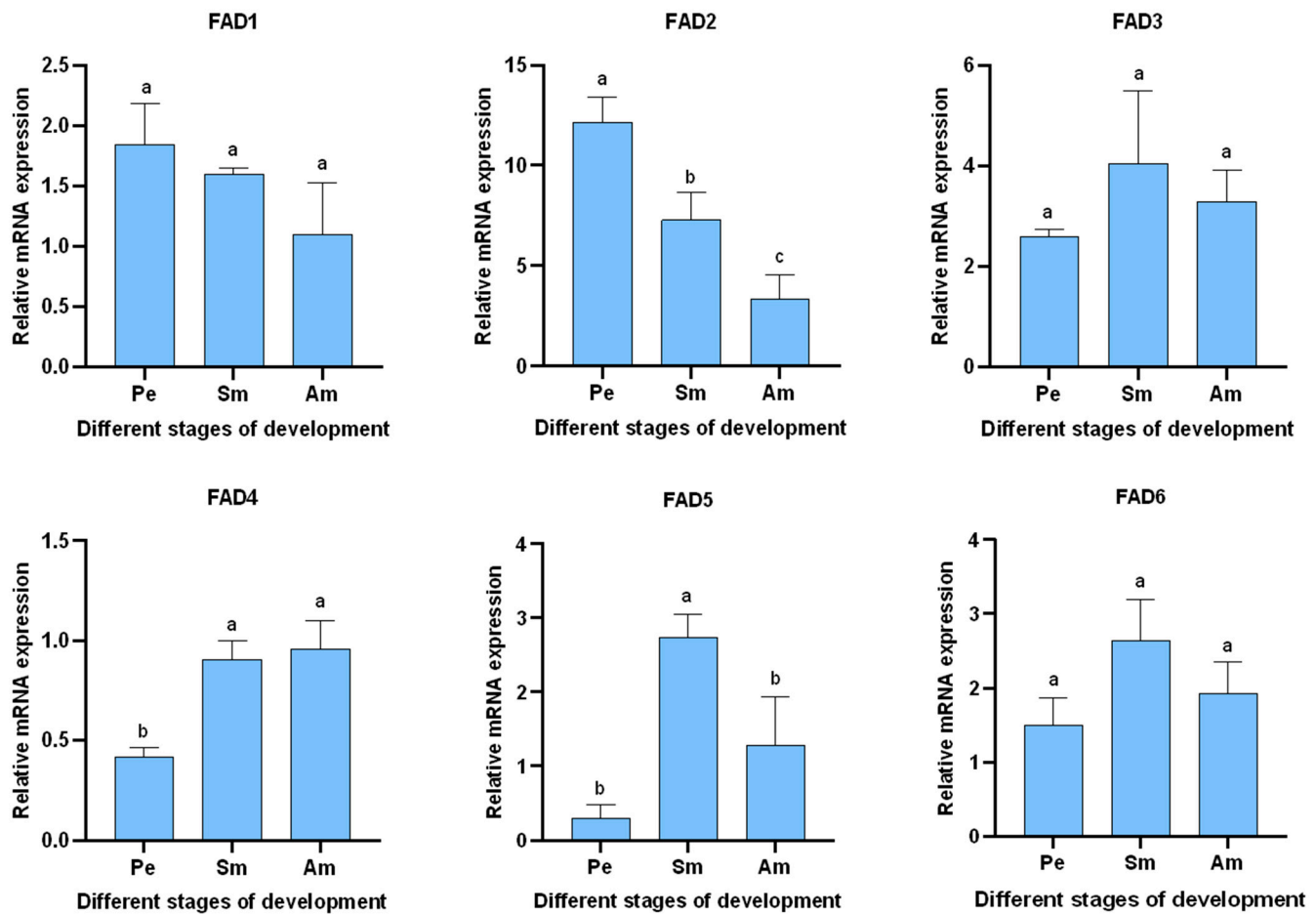


Figure 9. Expression profiles of *AglaFAD* genes in different stages of development. Note: Pe, primary eclosion; Sm, sexual maturity; Am, after mating. Letters above the error bars indicate significant differences between three stages ($p < 0.05$, LSD).

4. Discussion

Most insects utilize pheromones to accomplish species-specific mate recognition, and FAD is particularly important in the generation of pheromone components with structural diversity. However, the FAD gene family has only been characterized at the genomic level in some insects belonging to Diptera and Lepidoptera, such as *M. domestica* and *S. litura* [36,37], with no systematic analyses being focused on *A. glabripennis*.

In this study, searches of the whole genome of *A. glabripennis* using bioinformatics methods revealed six *AglaFAD* genes, which were unevenly distributed on four chromosomes. The deduced amino acid sequences of these genes exhibited three conserved histidine-rich sequences in the conserved arrangement characteristic of membrane-bound desaturases [3], with roughly the same conserved motifs, a relatively conserved central sequence, and a marked lack of homology between the N- and C-terminal portions [38]. All the proteins were hydrophilic and predicted to contain four–five transmembrane domains, identical to most eukaryotic fatty acid desaturases [39–41]. Subcellular localization prediction revealed that they mainly function in the endoplasmic reticulum, consistent with results for homologues in *Euzophera pyriella* (Yang, 1994) [42]; thus, these proteins conform to the model proposed by Stukey et al., in which the peptide chain spans the membrane four times and exposes the three histidine clusters on the cytoplasmic side of the endoplasmic reticulum [43]. In a phylogenetic analysis, FADs in *A. glabripennis* were assigned to two branches, with *AglaFAD*3–6 clustered on the $\Delta 9$ branch and *AglaFAD*1–2 clustered on the $\Delta 14$ branch, suggesting that they function at different positions in the carbon chain. Transcriptomic analysis of the closely related species *Helicoverpa assulta* (Guenée, 1852) on

the $\Delta 9$ branch clarified that the key gene for the sex pheromone component is *Des* [44]. In *Ostrinia scapulalis* (Walker, 1859) on the $\Delta 14$ branch, *Des* determines the ratio of the sex pheromone Z11–14:OAc and E11–14:OAc [45]. The *AglaFADs*, belonging to the same cluster, may have similar functions in pheromone synthesis.

Analyses of expression profiles in different tissues of male and female adults revealed that *AglaFAD2* and *AglaFAD5* are specifically expressed in female tissues, with relatively high expression in the wings and gonads of females. Based on the detection of contact pheromones at the wing base, it was hypothesized that *AglaFAD2* and *AglaFAD5* might be involved in the pheromone biosynthesis pathway in both the wings and the gonads of *A. glabripennis* [28]. *AglaFAD3* was mainly expressed in males, and the other three *AglaFADs* were expressed at different levels in other tissues of both sexes, suggesting that they regulate fatty acid synthesis in other tissues.

Comparative analyses of different developmental stages revealed that *AglaFAD2* and *AglaFAD5* tend to increase and then decrease during development in the wings of females, reaching the highest expression at sexual maturity. It is possible that, as females matured, they began to synthesize more of the contact pheromone to attract males, requiring more *FAD*, whereas the demand for the contact pheromone was reduced shortly after the completion of copulation, resulting in a gradual decrease in the *FAD* content. Unlike the trend in *AglaFAD5* expression, *AglaFAD2* expression was high during the rapid development of the gonads in primary eclosion. It is speculated that *AglaFAD2* functions in both gonadal development and contact pheromone synthesis in females, similar to *desat10* in *Nilaparvata lugens* (Stal, 1854), which is expressed in females in the primary eclosion period [46]. In summary, these two genes are predicted to play important roles in contact pheromone synthesis.

5. Conclusions

A. glabripennis is an important international quarantine pest, causing significant damage to poplar, willow and other tree species. The pheromones of *A. glabripennis* play an important role in the process of courtship and mating. Therefore, we studied the *FAD* genes involved in the biosynthesis of contact sex pheromones in females. In this study, six *FAD* genes were identified from *A. glabripennis* that were similar in conserved domains and sequences. Phylogenetic analysis divided them into two branches, showing that they function at different carbon locations in pheromone precursor substances. In addition, we provided detailed results of physicochemical properties, subcellular localization prediction, gene structure analysis, and conserved motif analysis of *FAD* genes and their coding proteins. Differences in the expression of *AglaFADs* in different tissues indicate their functional diversity. Among them, *AglaFAD2* and *AglaFAD5* were specifically expressed in females and reached a peak in the period of sexual maturity, suggesting that they may play a role in the biosynthesis of contact-sex pheromones in females. These results provide a theoretical basis for further analysis of the function of *AglaFAD* genes in female contact pheromone biosynthesis, helping to identify genetic targets and thus develop control strategies for *A. glabripennis*.

Supplementary Materials: The following supporting information can be downloaded at: <https://www.mdpi.com/article/10.3390/f15040690/s1>, File S1: 48 *FAD* amino acid sequences.

Author Contributions: Conceptualization, X.S. and J.T.; methodology, X.S. and Y.X. (Yabei Xu); software, X.S. and Y.X. (Yabei Xu); validation, Y.X. (Yu Xing) and M.L.; formal analysis, X.S.; investigation, X.S., Y.X. (Yabei Xu) and S.Z.; resources, X.S., Y.X. (Yabei Xu) and S.Z.; data curation, X.S. and M.L.; writing—original draft preparation, X.S.; writing—review and editing, S.Z., Y.X. (Yabei Xu), J.T. and F.H.; visualization, Y.X. (Yu Xing) and M.L.; supervision, F.H.; project administration, J.T.; funding acquisition, J.T. All authors have read and agreed to the published version of the manuscript.

Funding: This research was funded by the Chinese National Natural Science Foundation (32371886).

Data Availability Statement: The data are not publicly available due to the usage for ongoing project.

Acknowledgments: We are very grateful to Yurong Li, Lingxu Zhi, and the staff of Jiayuguan Forestry and Grassland Bureau for their kind assistance during the fieldwork.

Conflicts of Interest: The authors declare that this research was conducted in the absence of any commercial or financial relationships that could be construed as a potential conflict of interest.

References

- Helmkamp, M.; Cash, E.; Gadau, J. Evolution of the insect desaturase gene family with an emphasis on social Hymenoptera. *Mol. Biol. Evol.* **2015**, *32*, 456–471. [\[CrossRef\]](#) [\[PubMed\]](#)
- Zhang, S.D.; Li, X.; Bin, Z.; Du, M.F.; Yin, X.M.; An, S.H. Molecular identification of a pancreatic lipase-like gene involved in sex pheromone biosynthesis of *Bombyx mori*. *Insect Sci.* **2014**, *21*, 459–468. [\[CrossRef\]](#)
- Knipple, D.C.; Rpsenfield, C.L.; Nielsen, R.; You, K.M.; Jeong, S.E. Evolution of the integral membrane desaturase gene family in moths and flies. *Genetics* **2002**, *162*, 1737–1752. [\[CrossRef\]](#)
- Roelofs, W.L.; Rooney, A.P. Molecular genetics and evolution of pheromone biosynthesis in Lepidoptera. *Proc. Natl. Acad. Sci. USA* **2003**, *100*, 9179–9184. [\[CrossRef\]](#)
- Fang, S.; Ting, C.T.; Lee, C.R.; Chu, K.H.; Wang, C.C.; Tsaur, S.C. Molecular evolution and functional diversification of fatty acid desaturases after recurrent gene duplication in *Drosophila*. *Mol. Biol. Evol.* **2009**, *26*, 1447–1456. [\[CrossRef\]](#) [\[PubMed\]](#)
- Xue, B.Y.; Rooney, A.P.; Kajikawa, M.; Okada, N.; Roelofs, W.L. Novel sex pheromone desaturases in the genomes of corn borers generated through gene duplication and retroposon fusion. *Proc. Natl. Acad. Sci. USA* **2007**, *104*, 4467–4472. [\[CrossRef\]](#)
- Hashimoto, K.; Yoshizawa, A.C.; Okuda, S.; Kuma, K.; Goto, S.; Kanehisa, M. The repertoire of desaturases and elongases reveals fatty acid variations in 56 eukaryotic genomes. *J. Lipid Res.* **2008**, *49*, 183–191. [\[CrossRef\]](#) [\[PubMed\]](#)
- Keays, M.C.; Barker, D.; Wicker-Thomas, C.; Ritchie, M.G. Signatures of selection and sex-specific expression variation of a novel duplicate during the evolution of the *Drosophila* desaturase gene family. *Mol. Ecol.* **2011**, *20*, 3617–3630. [\[CrossRef\]](#)
- Marcillac, F.; Grosjean, Y.; Ferveur, J.F. A single mutation alters production and discrimination of *Drosophila* sex pheromones. *Proc. R. Soc. B-Biol. Sci.* **2005**, *272*, 303–309. [\[CrossRef\]](#)
- Shirangi, T.R.; Dufour, H.D.; Williams, T.M.; Carroll, S.B. Rapid evolution of sex pheromone-producing enzyme expression in *Drosophila*. *PLoS Biol.* **2009**, *7*, e1000168. [\[CrossRef\]](#)
- Ng, S.H.; Shankar, S.; Shikichi, Y.; Akasaka, K.; Moro, K.; Yew, J.Y. Pheromone evolution and sexual behavior in *Drosophila* are shaped by male sensory exploitation of other males. *Proc. Natl. Acad. Sci. USA* **2014**, *111*, 3056–3061. [\[CrossRef\]](#) [\[PubMed\]](#)
- Hagstrom, A.K.; Albre, J.; Tooman, L.K.; Thirmawithana, A.H.; Corcoran, J.; Löfstedt, C.; Newcomb, R.D. A novel fatty acyl desaturase from the pheromone glands of *Ctenopseustis obliquana* and *C. herana* with specific Z5-desaturase activity on myristic acid. *J. Chem. Ecol.* **2014**, *40*, 63–70. [\[CrossRef\]](#)
- Wang, B.; Lin, X.D.; Du, Y.J. Biosynthesis and endocrine regulation of sex pheromones in moth. *J. Appl. Ecol.* **2015**, *26*, 3235–3250.
- Smith, M.T.; Bancroft, J.; Li, G.; Gao, R.; Teale, S. Dispersal of *Anoplophora glabripennis* (Cerambycidae). *Environ. Entomol.* **2001**, *30*, 1036–1040. [\[CrossRef\]](#)
- Williams, D.W.; Lee, H.P.; Kim, I.K. Distribution and abundance of *Anoplophora glabripennis* (Coleoptera: Cerambycidae) in natural Acer stands in South Korea. *Environ. Entomol.* **2004**, *33*, 540–545. [\[CrossRef\]](#)
- Hérard, F.; Ciampitti, M.; Maspero, M.; Krehan, H.; Benker, U.; Boegel, C.; Schrage, R.; Bouhot-Delduc, L.; Bialooki, P. *Anoplophora* species in Europe: Infestations and management processes 1. *EPPO Bull.* **2006**, *36*, 470–474. [\[CrossRef\]](#)
- Carter, M.; Smith, M.; Harrison, R. Genetic analyses of the Asian longhorned beetle (Coleoptera, Cerambycidae, *Anoplophora glabripennis*), in North America, Europe and Asia. *Biol. Invasions* **2010**, *12*, 1165–1182. [\[CrossRef\]](#)
- Straw, N.A.; Fielding, N.J.; Tilbury, C.; Williams, D.T.; Cull, T. History and development of an isolated outbreak of Asian longhorn beetle *Anoplophora glabripennis* (Coleoptera: Cerambycidae) in southern England. *Agric. For. Entomol.* **2016**, *18*, 280–293. [\[CrossRef\]](#)
- Yan, J.J. Research on distribution of basicosta whitespotted longicorn in east China. *J. North-East. For. Coll. China* **1985**, *13*, 62–69.
- Wang, Z.G. *Study on the Occurrence Dynamics of Anoplophora glabripennis (Coleoptera: Cerambycidae) and Its Control Measures*; Northeast Forestry University: Harbin, China, 2004.
- Luo, Y.; Huang, J.; Li, J. Major achievements, problems and prospects of poplar longicorn beetles research in China. *Insect Knowl.* **2000**, *37*, 116–122.
- Hajek, A.E.; Huang, B.; Dubois, T.; Smith, M.T.; Li, Z. Field studies of control of *Anoplophora glabripennis* (Coleoptera: Cerambycidae) using fiber bands containing the entomopathogenic fungi *Metarhizium anisopliae* and *Beauveria brongniartii*. *Biocontrol Sci. Technol.* **2006**, *16*, 329–343. [\[CrossRef\]](#)
- Sun, Y.; Zhao, H.; Wang, Q.; Mei, W.; Liu, X. Research on the control technology of the Asian longhorned beetle. *For. Sci. Technol.* **2016**, *41*, 51–53.
- Zhu, N.; Zhang, D.Y.; Wu, L.P.; Hu, Q.; Fan, J.T. Attractiveness of aggregation pheromones and host plant volatiles to *Anoplophora glabripennis* and *A. chinensis* (Coleoptera: Cerambycidae). *J. Entomol.* **2017**, *60*, 421–430. [\[CrossRef\]](#)
- Xu, T.; Teale, S.A. Chemical ecology of the Asian longhorn beetle, *Anoplophora glabripennis*. *J. Chem. Ecol.* **2021**, *47*, 489–503. [\[CrossRef\]](#) [\[PubMed\]](#)
- Ginzel, M.D.; Hanks, L.M. Contact Pheromones as Mate Recognition Cues of Four Species of Longhorned Beetles (Coleoptera: Cerambycidae). *J. Insect Behav.* **2003**, *16*, 181–187. [\[CrossRef\]](#)

27. Wickham, J.D.; Xu, Z.C.; Teale, S.A. Evidence for a female-produced, long range pheromone of *Anoplophora glabripennis* (Coleoptera: Cerambycidae). *Insect Sci.* **2012**, *19*, 355–371. [[CrossRef](#)]
28. Li, D.J.; Tokoro, M.; Nacashima, T. Mechanism of mating action of *Anoplophora glabripennis* (Motsch.). *J. Beijing For. Univ.* **1999**, *21*, 33–36.
29. Zhang, A.J.; Oliver, J.E.; Chauhan, K.; Zhao, B.; Xia, L.; Xu, Z. Evidence for contact sex recognition pheromone of the Asian longhorned beetle, *Anoplophora glabripennis* (Coleoptera: Cerambycidae). *Naturwissenschaften* **2003**, *90*, 410–413. [[CrossRef](#)] [[PubMed](#)]
30. Blomquist, G.J.; Dillwith, J.W.; Adams, T.S. Biosynthesis and endocrine regulation of sex pheromone production in *Diptera*. In *Pheromone Biochemistry*; Academic Press: Cambridge, MA, USA, 1987; pp. 217–250. [[CrossRef](#)]
31. Latli, B.; Prestwich, G.D. Metabolically blocked analogs of housefly sex pheromone: I. Synthesis of alternative substrates for the cuticular monooxygenases. *J. Chem. Ecol.* **1991**, *17*, 1745–1768. [[CrossRef](#)]
32. Zhang, B.Y. *Identification of the Sex Pheromone Synthesis Genes of Spodoptera litura and Functional Study of Its Important Genes*; Shanxi University: Taiyuan, China, 2023.
33. Zhang, Y.N.; Zhu, X.Y.; Fang, L.P.; He, P.; Wang, Z.Q.; Chen, G.; Sun, L.; Ye, Z.F.; Deng, D.G.; Li, J.B. Identification and expression profiles of sex pheromone biosynthesis and transport related genes in *Spodoptera litura*. *PLoS ONE* **2015**, *10*, e0140019. [[CrossRef](#)]
34. Sayanova, O.; Shewry, P.R.; Napier, J.A. Histidine-41 of the cytochrome b5 domain of the borage delta6 fatty acid desaturase is essential for enzyme activity. *Plant Physiol.* **1999**, *121*, 641–646. [[CrossRef](#)] [[PubMed](#)]
35. Libisch, B.; Michaelson, L.V.; Lewis, M.J.; Shewry, P.R.; Napier, J.A. Chimeras of $\Delta 6$ Fatty Acid and $\Delta 8$ Sphingolipid Desaturases. *Biochem. Biophys. Res. Commun.* **2000**, *279*, 779–785. [[CrossRef](#)] [[PubMed](#)]
36. Eigenheer, A.L.; Young, S.; Blomquist, G.J.; Borgeson, C.E.; Tillman, J.A.; Tittiger, C. Isolation and molecular characterization of *Musca domestica* delta-9 desaturase sequences. *Insect Mol. Biol.* **2002**, *11*, 533–542. [[CrossRef](#)] [[PubMed](#)]
37. Rodríguez, S.; Hao, G.; Liu, W.; Piña, B.; Rooney, A.P.; Camps, F.; Roelofs, W.L.; Fabriàs, G. Expression and evolution of $\Delta 9$ and $\Delta 11$ desaturase genes in the moth *Spodoptera littoralis*. *Insect Biochem. Mol. Biol.* **2004**, *34*, 1315–1328. [[CrossRef](#)] [[PubMed](#)]
38. Lauritzen, L.; Hansen, H.S.; Jørgensen, M.H.; Michaelsen, K.F. The Essentiality of Long Chain N-3 Fatty Acids in Relation to Development and Function of the Brain and Retina. *Prog. Lipid Res.* **2001**, *40*, 1–94. [[CrossRef](#)]
39. Man, W.C.; Miyazaki, M.; Chu, K.; Ntambi, J.M. Membrane topology of mouse stearyl-CoA desaturase 1. *J. Biol. Chem.* **2006**, *281*, 1251–1260. [[CrossRef](#)] [[PubMed](#)]
40. Cao, W.R. Bioinformatics Analysis of the SCD Protein in Pig. *Anim. Feed. Sci.* **2014**, *35*, 5–7. [[CrossRef](#)]
41. Zhang, M.; Zhang, G.R. cDNA cloning and prokaryotic expression of acyl-CoA delta 9 desaturase from *Chrysomya megacephala* (Fabricius). *J. Environ. Entomol.* **2018**, *40*, 1306–1315.
42. Wang, D.G.; Ma, G.H.; He, P.P.; Xiong, R.C.; Cao, Y.; Zhang, P.; Han, X.; Yang, M.L. Gene Sequences and Expression Analysis of Fatty Acid $\Delta 9$ Desaturase of *Euzophera pyriella* during Different Stages. *Xinjiang Agric. Sci.* **2020**, *57*, 877–887. [[CrossRef](#)]
43. Stuke, J.E.; McDonough, V.M.; Martin, C.E. The *OLE1* gene of *Saccharomyces cerevisiae* encodes the delta 9 fatty acid desaturase and can be functionally replaced by the rat stearyl-CoA desaturase gene. *J. Biol. Chem.* **1990**, *265*, 20144–20149. [[CrossRef](#)]
44. Li, Z.Q.; Zhang, S.; Luo, J.Y.; Wang, C.Y.; Lv, L.M.; Dong, S.L.; Cui, J.J. Transcriptome comparison of the sex pheromone glands from two sibling *Helicoverpa* species with opposite sex pheromone components. *Sci. Rep.* **2015**, *5*, 9324. [[CrossRef](#)] [[PubMed](#)]
45. Sakai, R.; Fukuzawa, M.; Nakano, R.; Tatsuki, S.; Ishikawa, Y. Alternative suppression of transcription from two desaturase genes is the key for species-specific sex pheromone biosynthesis in two *Ostrinia* moths. *Insect Biochem. Mol. Biol.* **2009**, *39*, 62–67. [[CrossRef](#)] [[PubMed](#)]
46. Ye, W.F. *Characterization of the Biological Functions of Desaturase Nldesat10 and Salivary Protein NISEF1 of Brown Planthopper, Nilaparvata lugens*; Zhejiang University: Hangzhou, China, 2017.

Disclaimer/Publisher’s Note: The statements, opinions and data contained in all publications are solely those of the individual author(s) and contributor(s) and not of MDPI and/or the editor(s). MDPI and/or the editor(s) disclaim responsibility for any injury to people or property resulting from any ideas, methods, instructions or products referred to in the content.